The Effect of H-2 Partial Pressure on the Reaction Progression and Reversibility of Lithium-Containing Multicomponent Destabilized Hydrogen Storage Systems

8 AUTHORS, INCLUDING:

Thomas Christian Hansen
Institut Laue-Langevin
217 PUBLICATIONS **3,037** CITATIONS

SEE PROFILE

Dorthe B. Ravnsbæk
University of Southern Denmark
49 PUBLICATIONS **1,092** CITATIONS

SEE PROFILE

Torben Rene Jensen
Aarhus University
245 PUBLICATIONS **4,637** CITATIONS

SEE PROFILE

Gavin S Walker
University of Nottingham
131 PUBLICATIONS **3,509** CITATIONS

SEE PROFILE

The Effect of H_2 Partial Pressure on the Reaction Progression and Reversibility of Lithium-Containing Multicomponent Destabilized Hydrogen Storage Systems

Tobias E. C. Price,[†] David M. Grant,[‡] David Weston,[†] Thomas Hansen,[§] Lene M. Arnbjerg,[⊥] Dorthe B. Ravnsbæk,[⊥] Torben R. Jensen,[⊥] and Gavin S. Walker[*,†]

[†]Energy and Sustainability Research Division, and [‡]Materials, Mechanics and Structures Division, Engineering Faculty, The University of Nottingham, University Park, Nottingham, NG7 2RD, U.K.

[§]Institut Laue Langevin, 6 rue Jules Horowitz, BP 156, 38042 Grenoble cedex 9, France

[⊥]Center for Materials Crystallography, iNANO and Department of Chemistry, Aarhus University, Langelandsgade 140, DK-8000 Aarhus C, Denmark

ABSTRACT: It is known that the reaction path for the decomposition of $LiBH_4$: MgH_2 systems is dependent on whether decomposition is performed under vacuum or under a hydrogen pressure (typically 1–5 bar). However, the sensitivity of this multicomponent hydride system to partial pressures of H_2 has not been investigated previously. A combination of in situ powder neutron and X-ray diffraction (deuterides were used for the neutron experiments) have shed light on the effect of low partial pressures of hydrogen on the decomposition of these materials. Different partial pressures have been achieved through the use of different vacuum systems. It was found that all the samples decomposed to form Li–Mg alloys regardless of the vacuum system used or sample stoichiometry of the multicomponent system. However, upon cooling the reaction products, the alloys showed phase instability in all but the highest efficiency pumps (i.e., lowest base pressures), with the alloys reacting to form LiH and Mg. This work has significant impact on the investigation of Li-containing multicomponent systems and the reproducibility of results if different dynamic vacuum conditions are used, as this affects the apparent amount of hydrogen evolved (as determined by ex situ experiments). These results have also helped to explain differences in the reported reversibility of the systems, with Li-rich samples forming a passivating hydride layer, hindering further hydrogenation.

$Mg_{0.816}Li_{0.184} + 0.092H_2 \rightarrow 0.816Mg + 0.184LiH$
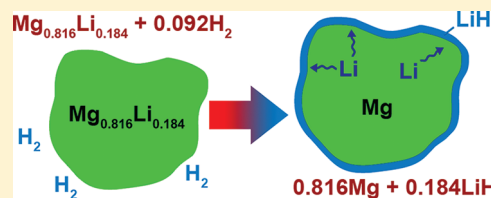
1. INTRODUCTION

A concerted investigation into alternatives to fossil fuels for mobile power generation has been undertaken worldwide in order to reduce our anthropogenic effects on the environment. The potential of hydrogen as an energy vector for mobile and small scale energy generation has led to challenging H_2 capacity targets. For automotive applications, a system target of 5.5 wt.% H_2 capacity by 2015 has been set by the US Department of Energy.[1] Light metal complex hydrides have been the source of many studies due to their high volumetric and gravimetric capacity. Complex hydrides based on $[AlH_4]^-$ and $[BH_4]^-$ anions ionically bonded to a light metal cation such as Li^+, Mg^{2+}, Na^+ give some of the highest achievable hydrogen storage capacities (viz., 18.5 wt.% for $LiBH_4$).[2] However, the high stability of many complex hydrides causes decomposition temperatures to be significantly higher than that required for automotive applications, e.g., $LiBH_4$ does not fully decompose until >600 °C.[3] Development of systems based on these complex hydrides for automotive applications requires the operating temperatures to be significantly reduced which may be achieved by thermodynamic destabilization of the system.[3–7] Addition of a destabilization reagent which leads to the formation of more stable end products will reduce the enthalpy for dehydrogenation, leading to a reduction in the decomposition temperature.

A widely investigated system is that of $LiBH_4$ combined with MgH_2; however, there have been inconsistencies in the reported reactions and the reversibility throughout the literature, depending on the decomposition environment, in particular when the decomposition was performed under vacuum.[5,6,8–11]

In situ structural characterization by synchrotron radiation powder X-ray diffraction (SR-PXD) or neutron diffraction (PND) has been key in probing the interplay between the components, varying the stoichiometry and reaction environment within the $LiBH_4$:MgH_2 system.[4,7,12–16] For decompositions performed under a hydrogen partial pressure at or above 1 bar, the system forms MgB_2 as shown in Scheme 1, as confirmed by in situ PND for both the 2:1 ratio and a magnesium-rich system with a 0.3:1 ratio[4] and in situ SR-PXD of the 2:1 ratio by Bosenberg et al.[12]

Under a dynamic vacuum environment, both $LiBH_4$:MgH_2 ratios were confirmed to decompose through a reaction originally proposed by Yu et al., Scheme 2,[3] forming the α- and β-alloys of Mg_xLi_{1-x} (where $x = 0.816$ and 0.70, respectively).[4,7]

Although there is consistency for the results reported by different laboratories for the reaction under $p(H_2) \geq 1$
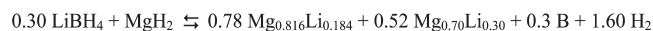
Scheme 1. Reaction Pathway when the Decomposition is under a Pressure

$$2LiBH_4 + MgH_2 \leftrightarrows 2LiH + MgB_2 + 4H_2$$
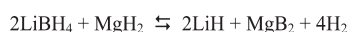
Scheme 2. Reaction Pathway when the Decomposition Is under a Dynamic Vacuum

$$0.30\ LiBH_4 + MgH_2 \leftrightarrows 0.78\ Mg_{0.816}Li_{0.184} + 0.52\ Mg_{0.70}Li_{0.30} + 0.3\ B + 1.60\ H_2$$

bar,[5,6,8−12,16] this is not the case for groups investigating the decomposition reaction under a dynamic vacuum. Some groups have not found evidence for the alloys, reporting instead formation of Mg metal and LiH, and for the 2:1 ratio, finding no reversibility for these end products.[5,6,8] In contrast, we have shown that hydrogenation of the alloy-containing end products have excellent reversibility and very fast kinetics.[4] Investigations in the literature have used varying pumping systems, of differing H_2 pumping efficiencies, which will affect the ultimate base pressure and hence the partial pressure of hydrogen into which the decompositions were performed. The results presented below represent a collation of data from our investigations into 0.3:1, 0.23:1, 0.44:1, and 2:1 ratios of MgH_2:$LiBH_4$, through PND and PXD in situ investigations. This has allowed us to investigate the effect of different pumping systems and the quality of the vacuum they produce upon the reaction pathways of these multicomponent systems.

2. EXPERIMENTAL METHODS

Three ratios of the $LiBH_4$:MgH_2 system were prepared for this study. The materials used were $LiBH_4$ (Acros Organics, 95%), $^7Li^{11}BD_4$ (Katchem, 98%), and MgH_2 (Alfar Aesar, 98%), the main impurities being limited to oxide and/or unhydrogenated products as characterized by PXD.[14] The latter was ball milled and subsequently cycled in deuterium (99.8%, D_2, BOC) at least two times to form MgD_2. All handling procedures were conducted under an inert atmosphere (<0.3 ppm H_2O/O_2). Mixtures (1.5 g) of $LiBD_4$:MgD_2 (0.3:1, 0.23:1, and 0.44:1 molar ratios) or $LiBH_4$:MgH_2 (0.3:1) were mechanically milled for 1 h under Ar gas at 300 rpm using a Fritsch Rotary P5 ball mill.

In situ experiments performed using PXD and PND are described below, the gas manifold systems are described in detail, the vacuum pumps attached to the manifold systems were commercial pumps which, like most commercial pumps, have little information on the pumping characteristics of hydrogen or deuterium. However, the base pressures achievable, directly above the pump, in hydrogen and deuterium are likely to be up to 2 orders of magnitude higher than that achievable in N_2 or Ar.[17] The pressure above the sample will also be affected by the conductance of the manifold system. This is discussed in relation to each vacuum system as detailed below.

In situ SR-PXD data were collected at the synchrotron MAX II, Lund, Sweden, in the research laboratories MAX-Lab at beamline I711 equipped with a MAR165 CCD detector system, using a selected wavelength of $\lambda = 1.09719$ Å.[18] The sample cell was developed specifically for studies of gas/solid reactions at high pressures and temperatures. The samples were mounted in a sapphire single crystal tube (1.09 mm o.d., 0.79 mm i.d., Al_2O_3) in an argon-filled glovebox (<0.1 ppm O_2, H_2O).[19] The gas manifold allowed high pressure hydrogen to be applied and evacuation of the sample via a rotary pump during X-ray data acquisition and is denoted as vacuum system A (VSA). For the VSA system, the ultimate pressure was measured to be between
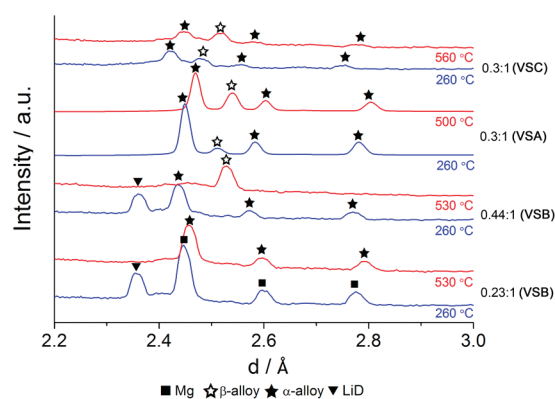

Figure 1. PXD and PND results for products of $LiBH_4$:MgH_2 samples decomposed under a dynamic vacuum followed by subsequent cooling to 260 °C. The sample stoichiometry and type of vacuum system used (VSA, VSB, or VSC) is indicated on the plot.

10^{-1} and 10^{-2} mbar measured next to the pump separated from the manifold by a low conductance pipe ($<10^{-4}\ ls^{-1}$).

The PND experiments were performed using the neutron diffractometer D20[20] at the Institute Laue-Langevin (ILL) in Grenoble, France ($\lambda = 2.42$ Å, flux $=4.2 \times 10^7$ n s^{-1} cm^{-2}). Data were analyzed using the Large Array Manipulation Program (LAMP) version 6. Samples of 1 g mass were packed into 316 L stainless steel vessels of 7 mm diameter i.d., with a length of 500 mm and sealed under argon gas. Deuteriding was performed via a gas manifold system connected to the sample, allowing application of >50 bar D_2 pressure at temperatures between 350 °C (0.23:1 and 0.44:1) and 400 °C (0.3:1). The PND manifold system is denoted vacuum system B (VSB) for experiments on 0.44:1 and 0.23:1 samples. VSB was pumped by a multistage roots pump (Adixen ACP-28) which had an ultimate pressure measured at the pump head of $>3 \times 10^{-2}$ mbar and connected to the manifold via piping of ca. 0.5 ls^{-1} conductance. A different vacuum system (VSC) was used on the 0.3:1 samples. In this case a scroll pump (Varian SH-110) of ultimate pressure of 6×10^{-2} mbar was connected directly to the manifold by a short flexible pipe of conductance ca. 2 ls^{-1}.

Diffraction peak areas were measured in order to follow the relative phase composition during the in situ experiments. The data presented has been collected using hydrogenated and deuterided samples. In order to simplify the text in both Results and Discussion, the word hydrogen and hydride will be used for both hydrogenated and deuterided samples, while the symbol H will denote both H and D. Figures will reflect the true isotope of the samples.

3. RESULTS

Mg-rich $LiBH_4$:MgH_2 samples with a molar ratio of 0.3:1, 0.23:1, and 0.44:1 were heated to above 500 °C until their fully dehydrogenated state was reached, i.e., until all the LiH had been decomposed to form Li–Mg alloys. The decomposition products were subsequently cooled, and the stability of the end products was assessed. Figure 1 shows the diffraction results for samples after decomposition at elevated temperatures and after subsequent cooling under vacuum to 260 °C. For the 0.3:1 sample, when decomposed under a vacuum generated by VSC, the end products at 560 °C contained α-alloy and β-alloy, and these phases were retained upon cooling to 260 °C; the diffraction lines had all shifted to smaller d-spacing as expected from the thermal expansion coefficient for these phases. However, for a 0.3:1 sample decomposed under vacuum generated by VSA, even though the decomposition products at 515 °C had the same two phases, α-alloy and β-alloy, after cooling to 260 °C the peak
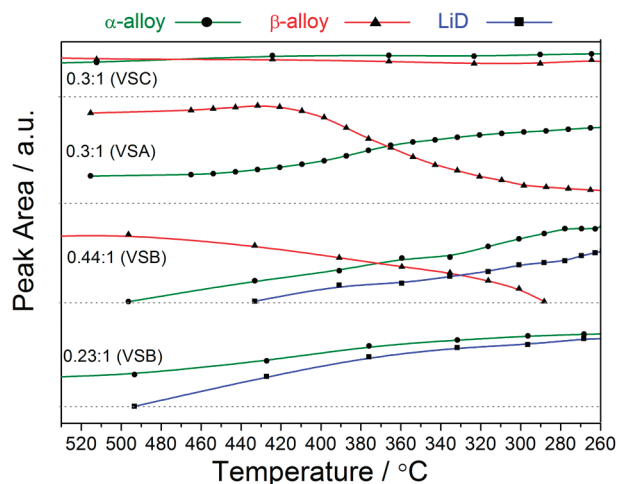
Figure 2. Sample composition as characterized by diffraction peak area analysis during the cooling of LiBH$_4$:MgH$_2$ samples while under vacuum generated by either a VSA, VSB, or VSC vacuum system.
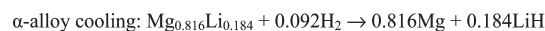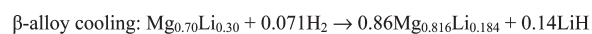
intensity had decreased for the β-alloy with an increase in intensity for the α-alloy pattern. For the more Li-rich 0.44:1 sample decomposed under a vacuum generated by VSB, only the β-alloy was identified at 530 °C, but after cooling to 260 °C the β-alloy was no longer evident and new phases of LiH and α-alloy had appeared in the NPD patterns. A more Li-deficient sample, 0.23:1 ratio, was also investigated under a vacuum generated by VSB, which formed the α-alloy evident at 530 °C, but once again after cooling to 260 °C the sample had formed LiH; however, this time the remaining metal was Mg and not an alloy.

Changes in the relative amounts of compounds was investigated using integrated diffracted intensities measured during cooling of the samples from >520 to 260 °C; see Figure 2. No change in phase was detected upon cooling the decomposed 0.3:1 sample when VSC was used to generate the vacuum. However, using VSA led to the β-alloy pattern reducing in intensity at ca. 430 °C with a concomitant rise in intensity of an α-alloy pattern. No XRD pattern was observed for a LiH phase during the cooling phase (nor in fact during the preceding decomposition). The decomposition products of 0.23:1 and 0.44:1 samples cooled under a VSC generated vacuum showed that in the more Li-rich 0.44:1 sample, the β-alloy pattern decreased in intensity, along with the appearance of an α-alloy phase at 500 °C and a LiH phase at 430 °C. By 260 °C, no β-alloy was detected, leaving only the α-alloy and LiH diffraction patterns for this sample. Upon cooling the more Mg-rich 0.23:1 sample, the initial α-alloy pattern increased in intensity at ca. 490 °C, along with the formation of a LiH phase, both patterns increasing in intensity as the sample was cooled to 260 °C.

4. DISCUSSION

The decomposition of the LiBH$_4$:MgH$_2$ samples under a dynamic vacuum forms Li−Mg alloys. As reported previously,[3,4] the LiH is destabilized by the presence of Mg, leading to the dehydrogenation of LiH at temperatures significantly below 600 °C. The resulting Mg$_x$Li$_{1-x}$ alloy(s) formed, as dictated by the binary Mg−Li phase diagram,[21] is illustrated in Scheme 2. From the results presented in Figure 1, the α-alloy (viz., Mg$_{0.816}$Li$_{0.184}$) and β-alloy (viz., Mg$_{0.70}$Li$_{0.30}$) were both formed

Scheme 3. Reaction Pathway during Partial Hydrogenation of the Mg Alloys

β-alloy cooling: $Mg_{0.70}Li_{0.30} + 0.071H_2 \rightarrow 0.86Mg_{0.816}Li_{0.184} + 0.14LiH$

α-alloy cooling: $Mg_{0.816}Li_{0.184} + 0.092H_2 \rightarrow 0.816Mg + 0.184LiH$

upon decomposition of the 0.3:1 system, because the ratio of Li to Mg is in the middle of a two-phase region in the alloy phase diagram. For the 0.23:1 sample, only an α-alloy phase was formed because the Li content was lower and remained within the single phase α region of the phase diagram. The more Li-rich 0.44:1 sample had sufficiently high Li content to take the alloy composition across into the single-phase β region of the phase diagram. These reactions were confirmed by the decomposition experiments regardless of the vacuum system used, so long as the sample was kept at an elevated temperature, > 500 °C, as shown in Figure 1.

The sample behavior upon cooling was as expected when VSC was used to provide the dynamic vacuum conditions, i.e., there was no change to the α- and β-alloy end products. This suggests that VSC provided a sufficiently low partial pressure of H$_2$, preventing hydrogenation of the Li upon cooling. In contrast, the sample cooled using VSA led to a significant change in the phases, with a loss of the β-alloy and a concomitant increase in the amount of α-alloy. This implies that the Li content available for the alloy system had decreased, which can only be explained by Li reacting with H$_2$ to form LiH. However, no LiH was observed in this PXD experiment, which is due to the fact that both Li and H have small X-ray scattering cross-sections and that the amount of LiH formed was beyond the detection limit of the experiment. In contrast, PND is inherently more sensitive to both elements,[22] allowing detection of a LiH phase for the 0.44:1 and 0.23:1 samples when cooled using VSB. Reaction upon cooling of the β-alloy with a low pressure of H$_2$ resulted in the formation of α-alloy and LiH, Scheme 3. The reaction of the α-alloy during cooling under a low pressure of H$_2$ caused formation of Mg and LiH, Scheme 3. It is possible that had the 0.44:1 sample been given enough time, all the Li within the remaining α-alloy would have reacted with the residual H$_2$ (so long as there was enough residual H$_2$ within the manifold).

For the 0.23:1 sample, the loss of Li from the α-alloy was inferred from the lack of change in the d-spacing for this phase upon cooling. One would have expected a significant decrease in the d-spacing due to thermal lattice contraction, but the expected lattice contraction from cooling was negated by the loss of Li from the lattice, which under isothermal conditions would result in a lattice expansion. Other supporting evidence is provided by the increase in peak area for the α-alloy pattern upon cooling, which is due to loss of Li from the alloy, which reduces the attenuation effect of Li presence due to its lower scattering cross section than that for Mg.[23]

The partial pressure over the sample for each of the vacuum systems employed was estimated to be of the order of 6×10^{-2} mbar up to 3 mbar for all three vacuum systems based on the poorer ultimate pressures expected for hydrogen.[17] However, from the results, VSC was clearly the only vacuum system with a base pressure lower than the equilibrium pressure for the hydrogenation of the Li−Mg alloys at 260 °C (i.e., preventing LiH formation upon cooling). Although all three vacuum systems had similar projected ultimate pressures for hydrogen, the scroll pump in VSC was directly attached to the manifold,

reducing outgassing from excess piping which may explain its lower base pressure. All three vacuum systems could deliver a base pressure higher than the hydrogenation equilibrium pressure at 500 °C, explaining why the alloys were formed above 500 °C regardless of the vacuum system employed. As the samples cooled, the plateau pressure for the alloys will eventually fall below the H_2 partial pressure that a given vacuum system can attain. No LiH was detected when VSC was used even upon cooling the sample to room temperature. This indicates that the temperature at which the plateau pressure is at a value below the back pressure from VSC must be lower than 260 °C and at a temperature where the kinetics are too slow for any significant hydrogenation to occur. Both VSA and VSB caused a higher H_2 partial pressure, enabling hydrogenation of the Li to occur upon cooling. The temperature at which hydrogenation starts for a given H_2 partial pressure gives an indication of the scale of thermodynamic destabilization for LiH by Mg.

For LiH, a temperature of 500 °C yields a plateau pressure of 3.5×10^{-2} mbar H_2, calculated from thermodynamic data in the literature;[24] therefore, the pressure attained by all the vacuum systems would need to be below this plateau pressure in order for LiH to decompose by 500 °C. None of the pumping systems used are able to achieve such a low pressure of hydrogen and are several orders of magnitude greater; thus, the LiH has been destabilized by Mg, leading to a lower ΔH of dehydrogenation. A rough calculation of the enthalpy of dehydrogenation can be made from the equation $\Delta H = \Delta ST - RT \ln p$; assuming the LiH entropy is the same for the destabilized system and that the minimum H_2 partial pressure for the vacuum systems is estimated as 3 mbar H_2, then this would equate to a reduction in ΔH from 181 kJ mol^{-1} H_2 to ≤ 152 kJ mol^{-1} H_2 to enable dehydrogenation above 500 °C. This equates to a heat of formation of 2.6 kJ mol^{-1} for $Mg_{0.816}Li_{0.184}$ which agrees well with the values reported in the literature 3.3 kJ mol^{-1}.[25]

These results help us to understand the apparent disparity within the literature for reported decomposition products under vacuum and inert gas conditions for the $LiBH_4$:MgH_2 system. In addition to experiments run under dynamic vacuum where the H_2 partial pressure will be dependent on the pump and manifold, many results are reported for products formed after temperature-programmed experiments which use a flowing inert gas (e.g., differential scanning calorimetry and thermal gravimetric analysis). Experiments using a flowing inert gas continually remove any hydrogen produced during the experiment; thus, there will be no H_2 partial pressure and hence would be analogous to an ultrahigh vacuum system. This helps to explain the difference in the results for Yu et al.[3] who identified the Mg_xLi_{1-x} alloys in the products from DSC run under an Ar carrier gas compared to Vajo et al.[5] who found LiH and Mg products after decomposing under a vacuum. The results shown above would suggest that Vajo et al. also formed the alloy products at 450 °C, but these hydrided upon cooling due to the residual H_2 partial pressure.

Another discrepancy between the two results is that when the end products for a 2:1 sample were LiH and Mg, these could not be hydrogenated to reform the $LiBH_4$,[5] but our earlier work has clearly shown that $LiBH_4$ can be reformed from the end products containing Mg + LiH or Mg_xLi_{1-x} alloys.[4] However, for the high Li-content 2:1 system, formation of a LiH passivating layer at the surface of Mg during hydrogenation caused a significant decrease in the reaction kinetics, yielding minimal MgH_2 formation under 90 bar H_2 at 400 °C.[4] These results indicate the importance of in situ characterization techniques in fully understanding the reactions that occur during an experiment. It also shows a surprising effect related merely to the pumping efficiency of a system and the care needed in interpreting reaction paths only based on ex situ characterization techniques. The hydrogenation effect observed due to the partial pressure of H_2 while cooling a sample can be expected for other Li-containing systems and those containing similarly reactive metals. We have not discussed static vacuum conditions, because such experiments will not be under vacuum once the sample starts to dehydrogenate and the partial pressure normally quickly rises to several bar depending on the size of the sample and the manifold; thus, virtually all the dehydrogenation occurs under a significant hydrogen pressure.

5. CONCLUSIONS

The results presented here demonstrate the sensitivity of $LiBH_4$:MgH_2 systems to subtle changes in hydrogen partial pressure under dynamic vacuum conditions, influencing whether the decomposition products are either retained upon cooling or form LiH. The work also shows that LiH was thermodynamically destabilized by Mg, forming the Li–Mg alloys, reducing ΔH by 29 kJ mol^{-1} H_2.

These results offer an explanation for the apparent disparity between reported reaction pathways in the literature for samples decomposed under inert conditions. Clearly, inert conditions for H_2-sensitive materials require either decomposition under an inert flowing gas or a dynamic vacuum system achieving a sufficiently low H_2 partial pressure. These findings highlight the important role of in situ structural characterization when following phase progressions, particularly when evolved phases may be dependent on partial pressures of H_2 and changing temperature. The in situ experiments show how the end products, formed at temperature, can differ from those after cooling; hence, ex situ experiments can in some instance unintentionally lead to the wrong reaction pathway being proposed. These results also show the importance of continuity between reaction environments when investigating samples through a range of techniques, not just diffraction experiments, e.g. using a flowing inert carrier gas such as DSC and TGA.

■ AUTHOR INFORMATION

Corresponding Author
Gavin.walker@nottingham.ac.uk

■ REFERENCES

(1) Dilich, S. Annual Merit Review and Peer Evaluation Meeting, US Department of Energy, Arlington, VA, May, 2009.

(2) Schlesinger, H. I.; Brown, H. C. *J. Am. Chem. Soc.* **1940**, *62*, 3429.

(3) Yu, X. B.; Grant, D. M.; Walker, G. S. *Chem. Commun. (Cambridge, U. K.)* **2006**, 3906.

(4) Price, T. E. C.; Grant, D. M.; Legrand, V.; Walker, G. S. *Int. J. Hydrogen Energy* **2010**, *35*, 4154.

(5) Vajo, J. J.; Skeith, S. L.; Mertens, F. *J. Phys. Chem. B* **2005**, *109*, 3719.

(6) Pinkerton, F. E.; Meyer, M. S.; Meisner, G. P.; Balogh, M. P.; Vajo, J. J. *J. Phys. Chem. C* **2007**, *111*, 12881.

(7) Walker, G. S.; Grant, D. M.; Price, T. E. C.; Legrand, V.; Yu, X. *J. Power Sources* **2009**, *189*, 902.

(8) Nakagawa, T.; Ichikawa, T.; Hanada, N.; Kojima, Y.; Fujii, H. *J. Alloys Compd.* **2007**, *446−447*, 306.

(9) Fan, M.-Q.; Sun, L.-X.; Zhang, Y.; Xu, F.; Zhang, J.; Chu, H.-l. *Int. J. Hydrogen Energy* **2008**, *33*, 74.

(10) Mao, J. F.; Wu, Z.; Chen, T. J.; Weng, B. C.; Xu, N. X.; Huang, T. S.; Guo, Z. P.; Liu, H. K.; Grant, D. M.; Walker, G. S.; Yu, X. B. *J. Phys. Chem. C* **2007**, *111*, 12495.

(11) Wang, P.-J.; Fang, Z.-Z.; Ma, L.-P.; Kang, X.-D.; Wang, P. *Int. J. Hydrogen Energy* **2008**, *33*, 5611.

(12) Bosenberg, U.; Doppiu, S.; Mosegaard, L.; Barkhordarian, G.; Eigen, N.; Borgschulte, A.; Jensen, T. R.; Cerenius, Y.; Gutfleisch, O.; Klassen, T.; Dornheim, M.; Bormann, R. *Acta Mater.* **2007**, *55*, 3951.

(13) Mosegaard, L.; Moller, B.; Jorgensen, J. E.; Filinchuk, Y.; Cerenius, Y.; Hanson, J. C.; Dimasi, E.; Besenbacher, F.; Jensen, T. R. *J. Phys. Chem. C* **2008**, *112*, 1299.

(14) Price, T. E. C.; Grant, D. M.; Telepeni, I.; Yu, X. B.; Walker, G. S. *J. Alloys Compd.* **2009**, *472*, 559.

(15) Price, T. E. C.; Grant, D. M.; Walker, G. S. In *Materials Innovations in an Emerging Hydrogen Economy*; George, G.; Wicks, J. S., Eds.; John Wiley & Sons Ltd,: Hoboken, New Jersey, USA, 2009; p 97.

(16) Bösenberg, U.; Kim, J. W.; Gosslar, D.; Eigen, N.; Jensen, T. R.; von Colbe, J. M. B.; Zhou, Y.; Dahms, M.; Kim, D. H.; Günther, R.; Cho, Y. W.; Oh, K. H.; Klassen, T.; Bormann, R.; Dornheim, M. *Acta Mater.* **2010**, *58*, 3381.

(17) In, S. R. *Vacuum* **2009**, *84*, 689.

(18) Cerenius, Y.; Stahl, K.; Svensson, L. A.; Ursby, T.; Oskarsson, A.; Albertsson, J.; Liljas, A. *J. Synchrotron Radiat.* **2000**, *7*, 203.

(19) Jensen, T. R.; Nielsen, T. K.; Filinchuk, Y.; Jørgensen, J. E.; Cerenius, Y.; Gray, E.; Webb, C. *J. Appl. Crystallogr.* **2010**, *43*, 1456.

(20) Hansen, T. C.; Henry, P. F.; Fischer, H. E.; Torregrossa, J.; Convert, P. *Meas. Sci. Technol.* **2008**, 034001.

(21) Butts, D. A.; Gale, W. F.; Totemeier, T. C. In *Smithells Metals Reference Book*, 8th ed.; Butterworth-Heinemann: Oxford, 2004; p 1.

(22) Munter, A. *Neutron News* **1992**, *3*, 29.

(23) Sears, V. *Neutron News* **1992**, *3*, 26.

(24) Lide, D. *CRC Handbook of Chemistry and Physics*, 88th ed.; CRC: Boca Raton, FL, 2007.

(25) Liang, C. P.; Gong, H. R. *J. Alloys Compd.* **2009**, *489*, 130.